High-frequency acousto-optic effects in Bragg reflectors

D. J. Farmer,[1] A. V. Akimov,[1] N. A. Gippius,[2] J. Bailey,[1] J. S. Sharp,[1,3] and A. J. Kent[1,*]

[1]*School of Physics and Astronomy, University of Nottingham, Nottingham, NG7 2RD, UK*
[2]*Skolkovo Institute of Science and Technology, Moscow Region, 143025, Russia*
[3]*Nottingham Nanotechnology and Nanoscience Centre, University of Nottingham, Nottingham, NG7 2RD, UK*
[*]*anthony.kent@nottingham.ac.uk*

Abstract: Picosecond acoustic interferometry was used to study the acousto-optic properties of a distributed Bragg reflector (DBR) manufactured from two immiscible polymers (cellulose acetate and polyvinylcarbyzole). Picosecond strain pulses were injected into the structure and changes in its reflectance were monitored as a function of time. The reflectance exhibited single-frequency harmonic oscillations as the strain pulse traversed the DBR. A transfer matrix method was used to model the reflectance of the DBR in response to interface modulation and photo-elastic effects. This work shows that photo-elastic effects can account for the acousto-optic response of DBRs with acoustically matched layers.

OCIS codes: (320.0320) Ultrafast optics; (160.0160) Materials; (310.0310) Thin films; (140.0140) Lasers and laser optics.

References and links

1. C. Colvard, R. Merlin, M. V. Klein, and A. C. Gossard, "Observation of folded acoustic phonons in a semiconductor superlattice," Phys. Rev. Lett. **45**(4), 298–301 (1980).
2. B. Jusserand, D. Paquet, F. Mollot, F. Alexandre, and G. Le Roux, "Influence of the supercell structure on the folded acoustical Raman line intensities in superlattices," Phys. Rev. B Condens. Matter **35**(6), 2808–2817 (1987).
3. T. Gorishnyy, C. K. Ullal, M. Maldovan, G. Fytas, and E. L. Thomas, "Hypersonic phononic crystals," Phys. Rev. Lett. **94**(11), 115501 (2005).
4. W. Cheng, J. J. Wang, U. Jonas, G. Fytas, and N. Stefanou, "Observation and tuning of hypersonic bandgaps in colloidal crystals," Nat. Mater. **5**(10), 830–836 (2006).
5. J. Groenen, F. Poinsotte, A. Zwick, C. M. Sotomayor-Torres, M. Prunnila, and J. Ahopelto, "Inelastic light scattering by longitudinal acoustic phonons in thin silicon layers: From membranes to silicon-on-insulator structures," Phys. Rev. B **77**(4), 045420 (2008).
6. X. Zhang, R. Sooryakumar, A. G. Every, and M. H. Manghnani, "Observation of organ-pipe acoustic excitations in supported thin films," Phys. Rev. B **64**, 081402(R) (2001).
7. P. Dainese, P. St. J. Russell, G. S. Wiederhecker, N. Joly, H. L. Fragnito, V. Laude, and A. Khelif, "Raman-like light scattering from acoustic phonons in photonic crystal fiber," Opt. Express **14**(9), 4141–4150 (2006).
8. G. S. Wiederhecker, A. Brenn, H. L. Fragnito, and P. St. J. Russell, "Coherent control of ultrahigh-frequency acoustic resonances in photonic crystal fibers," Phys. Rev. Lett. **100**(20), 203903 (2008).
9. J.-C. Beugnot and V. Laude, "Electrostriction and guidance of acoustic phonons in optical fibers," Phys. Rev. B **86**(22), 224304 (2012).
10. S. Gröblacher, K. Hammerer, M. R. Vanner, and M. Aspelmeyer, "Observation of strong coupling between a micromechanical resonator and an optical cavity field," Nature **460**(7256), 724–727 (2009).
11. Q. Lin, J. Rosenberg, D. Chang, R. Camacho, M. Eichenfield, K. J. Vahala, and O. Painter, "Coherent mixing of mechanical excitations in nano-optomechanical structures," Nat. Photonics **4**(4), 236–242 (2010).
12. S. Weis, R. Rivière, S. Deléglise, E. Gavartin, O. Arcizet, A. Schliesser, and T. J. Kippenberg, "Optomechanically Induced Transparency," Science **330**(6010), 1520–1523 (2010).
13. L. Ding, C. Baker, P. Senellart, A. Lemaitre, S. Ducci, G. Leo, and I. Favero, "High frequency GaAs nano-optomechanical disk resonator," Phys. Rev. Lett. **105**(26), 263903 (2010).
14. A. H. Safavi-Naeini, T. P. M. Alegre, M. Winger, and O. Painter, "Optomechanics in an ultrahigh-Q two-dimensional photonic crystal cavity," Appl. Phys. Lett. **97**(18), 181106 (2010).

#205467 - $15.00 USD Received 24 Jan 2014; revised 21 Mar 2014; accepted 23 Mar 2014; published 13 Jun 2014

15. A. Fainstein, N. D. Lanzillotti-Kimura, B. Jusserand, and B. Perrin, "Strong optical-mechanical coupling in a vertical GaAs/AlAs microcavity for subterahertz phonons and near-infrared light," Phys. Rev. Lett. **110**(3), 037403 (2013).
16. O. Arcizet, P.-F. Cohadon, T. Briant, M. Pinard, and A. Heidmann, "Radiation-pressure cooling and optomechanical instability of a micromirror," Nature **444**(7115), 71–74 (2006).
17. J. D. Teufel, T. Donner, D. Li, J. W. Harlow, M. S. Allman, K. Cicak, A. J. Sirois, J. D. Whittaker, K. W. Lehnert, and R. W. Simmonds, "Sideband cooling of micromechanical motion to the quantum ground state," Nature **475**(7356), 359–363 (2011).
18. J. Chan, T. P. M. Alegre, A. H. Safavi-Naeini, J. T. Hill, A. Krause, S. Gröblacher, M. Aspelmeyer, and O. Painter, "Laser cooling of a nanomechanical oscillator into its quantum ground state," Nature **478**(7367), 89–92 (2011).
19. I. S. Grudinin, H. Lee, O. Painter, and K. J. Vahala, "Phonon laser action in a tunable two-level system," Phys. Rev. Lett. **104**(8), 083901 (2010).
20. I. Mahboob, K. Nishiguchi, A. Fujiwara, and H. Yamaguchi, "Phonon lasing in an electromechanical resonator," Phys. Rev. Lett. **110**(12), 127202 (2013).
21. J. Sapriel, *Acousto-Optics* (John Wiley, 1979).
22. O. Matsuda and O. B. Wright, "Reflection and transmission of light in multilayers perturbed by picosecond strain pulse propagation," J. Opt. Soc. Am. B **19**(12), 3028–3041 (2002).
23. O. Matsuda, O. B. Wright, D. H. Hurley, V. Gusev, and K. Shimizu, "Coherent shear phonon generation and detection with picosecond laser acoustics," Phys. Rev. B **77**(22), 224110 (2008).
24. J. D. Joannopoulos, S. G. Johnson, J. N. Winn, and R. D. Meade, *Photonic Crystals: Molding the Flow of Light*, 2nd ed. (Princeton University, 2008).
25. M. Maldovan, "Sound and heat revolutions in phononics," Nature **503**(7475), 209–217 (2013).
26. A. S. Salasyuk, A. V. Scherbakov, D. R. Yakovlev, A. V. Akimov, A. A. Kaplyanskii, S. F. Kaplan, S. A. Grudinkin, A. V. Nashchekin, A. B. Pevtsov, V. G. Golubev, T. Berstermann, C. Brüggemann, M. Bombeck, and M. Bayer, "Filtering of elastic waves by opal-based hypersonic crystal," Nano Lett. **10**(4), 1319–1323 (2010).
27. Y. Pennec, B. Djafari Rouhani, E. H. El Boudouti, C. Li, Y. El Hassouani, J. O. Vasseur, N. Papanikolaou, S. Benchabane, V. Laude, and A. Martinez, "Simultaneous existence of phononic and photonic band gaps in periodic crystal slabs," Opt. Express **18**(13), 14301–14310 (2010).
28. H. N. Lin, R. J. Stoner, H. J. Maris, and J. Tauc, "Phonon attenuation and velocity measurements in transparent materials by picosecond acoustic interferometry," J. Appl. Phys. **69**(7), 3816–3822 (1991).
29. O. B. Wright, "Thickness and sound velocity measurement in thin transparent films with laser picosecond acoustics," J. Appl. Phys. **71**(4), 1617–1629 (1992).
30. C. Thomsen, H. T. Grahn, H. J. Maris, and J. Tauc, "Surface generation and detection of phonons by picosecond light pulses," Phys. Rev. B Condens. Matter **34**(6), 4129–4138 (1986).
31. O. B. Wright, "Ultrafast nonequilibrium stress generation in gold and silver," Phys. Rev. B Condens. Matter **49**(14), 9985–9988 (1994).
32. G. Tas and H. J. Maris, "Electron diffusion in metals studied by picosecond ultrasonics," Phys. Rev. B Condens. Matter **49**(21), 15046–15054 (1994).
33. H.-Y. Hao and H. J. Maris, "Dispersion of the long-wavelength phonons in Ge, Si, GaAs, quartz, and sapphire," Phys. Rev. B **63**(22), 224301 (2001).
34. J. W. Tucker and V. W. Rampton, *Microwave Ultrasonics in Solid State Physics* (North Holland, 1972).
35. J. Bailey and J. S. Sharp, "Infrared dielectric mirrors based on thin film multilayers of polystyrene and polyvinylpyrrolidone," J. Polym. Sci., B, Polym. Phys. **49**(10), 732–739 (2011).
36. C. C. Katsidis and D. I. Siapkas, "General transfer-matrix method for optical multilayer systems with coherent, partially coherent, and incoherent interference," Appl. Opt. **41**(19), 3978–3987 (2002).
37. A. V. Akimov, E. S. K. Young, J. S. Sharp, V. Gusev, and A. J. Kent, "Coherent hypersonic closed-pipe organ like modes in supported polymer films," Appl. Phys. Lett. **99**(2), 021912 (2011).
38. C. J. Morath and H. J. Maris, "Phonon attenuation in amorphous solids studied by picosecond ultrasonics," Phys. Rev. B Condens. Matter **54**(1), 203–213 (1996).
39. P. M. Walker, J. S. Sharp, A. V. Akimov, and A. J. Kent, "Coherent elastic waves in a one-dimensional polymer hypersonic crystal," Appl. Phys. Lett. **97**(7), 073106 (2010).
40. T. Czerniuk, C. Brüggemann, J. Tepper, S. Brodbeck, C. Schneider, M. Kamp, S. Höfling, B. A. Glavin, D. R. Yakovlev, A. V. Akimov, and M. Bayer, "Controlled lasing from active optomechanical resonators," http://arxiv.org/abs/1401.4359.
41. C. Brüggemann, A. V. Akimov, A. V. Scherbakov, M. Bombeck, C. Schneider, S. Hofling, A. Forchel, D. R. Yakovlev, and M. Bayer, "Laser mode feeding by shaking quantum dots in a planar microcavity," Nat. Photonics **6**(1), 30–34 (2012).
42. Y. Léger, "Double magic coincidence in an optomechanical laser cavity," Physics **6**, 6 (2013).

1. Introduction

The interaction of acoustic and electromagnetic waves in solids has been a topic of intense study since the beginning of the 20th century and has resulted in many practical applications,

#205467 - $15.00 USD Received 24 Jan 2014; revised 21 Mar 2014; accepted 23 Mar 2014; published 13 Jun 2014

such as acousto-optical modulators, filters and deflectors. During the last decade, the field of acousto-optics has progressed to include studies of nanometer scale objects, aimed at exploiting acoustic waves in nano-photonic and opto-mechanical devices. Traditional Brillouin scattering experiments have, so far, provided basic information about the acoustic spectra and the strength of acousto-optical interactions in various nanostructures [1–6]. In addition, acousto-optical effects excited in optical fibers provide the possibility of gigahertz (GHz) light modulation [7–9]. Another rapidly developing field concerns structures which exhibit both optical and acoustic resonances [10–15] and which demonstrate exciting phenomena such as optical cooling [16–18] and stimulated sound emission [19,20].

The mechanisms governing the interaction of light with high-frequency (GHz and THz) phonons in photonic nanostructures are still under debate and, as such, are the subject of much of the current research into high-frequency acousto-optics. Generally, the photoelastic effect (i.e. the dependence of the permittivity of a material on strain, induced by an acoustic wave) is considered to be the most important mechanism in transparent bulk solids with momentum conservation between the acoustic and electromagnetic waves governing various acousto-optical phenomena [21]. In complex nanostructures, like multilayered thin films, acoustic waves also modulate the positions of the internal interfaces and the size of the domains in the structure [22,23]. Such dynamic changes, which occur at the frequency of the acoustic wave, modulate the way that light interferes inside the structure. These in turn result in the modulation of the optical properties of the nanostructure as a whole. The interplay between the photoelastic effect and interface modulation determines the final optical output (e.g. reflection, transmission, scattering and the localization of photons) that is induced by acoustic waves in such a nanophotonic device. For strong interactions to occur between photons and phonons in nanophotonic devices, the wavelengths of the sound and light must be comparable. To produce acousto-optic devices that operate in the visible range of wavelengths requires materials that are structured on the 10-100 nm length scale and which typically have acoustic vibrational frequencies of ~10 GHz.

A particular branch of the current research in this area concerns periodic nanostructures with photonic stop bands (PSBs) [24]. The periodic nature of these structures means that they can also exhibit *phononic* stop bands, if the spatial variations in the acoustic properties of the structure occur on length scales comparable to the acoustic wavelength. With careful design, such structures may confine both optical and acoustic waves simultaneously, leading to a significant enhancement of the interactions between photons and phonons [15,25]. In practice, however, this situation is hard to achieve as producing structures which possess both complete photonic and phononic stop bands is a technically complex task [26]. Theoretical works in this area are mostly limited to calculations of dispersion relations for photonic-phononic crystals [27]. An example of experimentally studied 1D structures, includes acoustically induced modulations of the optical reflectance in a high-quality planar micro-cavity [15]. These modulations were shown to increase in strength when the optical wavelength corresponds to that of the cavity mode. The reported observations suggest realistic prospects for various advanced, high-frequency applications.

The majority of current nano-photonic devices (e.g. lasers, nano-cavities, and interferometers) require distributed Bragg reflectors (DBRs) as elements of the device. DBRs are multilayered periodic films, that are often classified as 1D photonic crystals [24]. DBRs characteristically possess PSBs and their optical properties have been studied in detail. However, no experimental or theoretical works considering the high-frequency acousto-optical properties of DBRs currently exist. It is not clear how acousto-optical interactions inside a DBR differ when compared to a homogeneous film of the same thickness and mean refractive index. What is clear, is that this is not trivial, even for the simplest case, when the acoustic dispersion is linear and phononic stop-bands do not exist. It is this issue that has motivated the present work, where acousto-optical effects inside a polymer DBR are studied using picosecond acoustic methods.

#205467 - $15.00 USD Received 24 Jan 2014; revised 21 Mar 2014; accepted 23 Mar 2014; published 13 Jun 2014

The main aim of the present work is to characterize coherent photo-elastic effects in a polymer based DBR where no acoustic mismatch exists between the layers using both experimental and theoretical methods. In this paper, the results of experiments where picosecond strain pulses were injected into DBR structures are presented. The pulses were monitored as they travelled through the multilayer structure by measuring the temporal evolution of the optical reflectance at a wavelength in the vicinity of the PSB. This technique, which is described in detail below is often called "picosecond acoustic interferometry" and has been widely used to study the acoustic properties of homogeneous and transparent solid films [28,29] and multilayers [22,23]. The work presented here shows that photo-elastic effects are sufficient to describe the acousto-optical properties of the DBRs studied. However, our analysis also shows that the modulation of the interfaces inside the DBR can contribute to the reflectance changes. In this case, the relative contributions of photo-elastic effect and interface modulation effects depend upon the wavelength, angle of incidence and polarization of the optical probe beam.

2. Picosecond acoustic interferometry

Firstly, we consider the simplest case of a homogeneous transparent dielectric film. We then extend our discussion to include the case of a DBR, thus allowing qualitative predictions of the expected behavior of our DBR sample to be made.

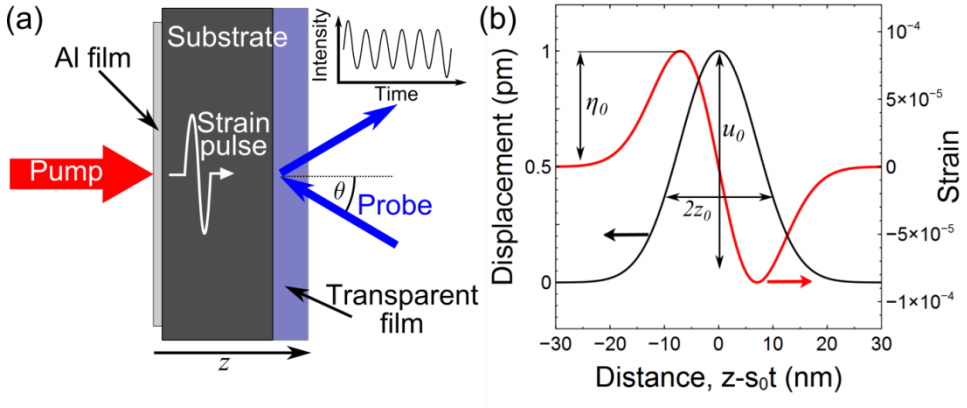

Fig. 1. (a) Diagram showing the experimental setup used to perform picosecond acoustic interferometry. The inset shows an example output signal where the reflected probe intensity is modulated by the strain pulse. (b) The expected Gaussian shape of the displacement pulse (black, solid line) and the associated strain (red line). The values shown on the axes correspond to the experimental conditions described in section 3.

A diagram of the experimental setup for measuring a transparent sample deposited on a crystalline substrate is shown in Fig. 1(a). Picosecond strain pulses are generated by a pulsed optical excitation of an aluminum (Al) film, deposited on the back side of the substrate [30]. These strain pulses are injected into the substrate where they propagate in the *z*-direction with the velocity of longitudinal sound until they reach the transparent film. The strain pulse is partially transmitted into the film and propagates through with a longitudinal sound velocity, s_0. The spatial/temporal evolution of the displacement, $u_z(z\text{-}s_0t)$, and strain, $\eta_{zz}(z\text{-}s_0t)$, pulses shown in Fig. 1(b) may, in practice, be described by a Gaussian function and its derivative respectively:

#205467 - $15.00 USD Received 24 Jan 2014; revised 21 Mar 2014; accepted 23 Mar 2014; published 13 Jun 2014

$$u_z(z') = u_0 \exp\left(-\frac{z'^2}{z_0^2}\right)$$
$$\eta_{zz}(z') = \frac{du_z}{dz} = -\frac{2u_0 z'}{z_0^2}\exp\left(-\frac{z'^2}{z_0^2}\right) \quad (1)$$

where $z' = z - s_0 t$ is the reduced coordinate, z_0 is a parameter which characterizes the width of the displacement pulses and u_0 is its amplitude [see Fig. 1(b)]. The strain pulse, $\eta_{zz}(z\text{-}s_0t)$, has an anti-symmetric shape with an amplitude, $\eta_0 = 1.2u_0/z_0$, and the spatial interval between the minimum and maximum points is $\sqrt{2}z_0$. The values of z_0, u_0 and η_0, shown schematically in Fig. 1(b), depend on the optical pump excitation conditions and the properties of both the substrate and the film. Typically, for solid substrates like sapphire or silicon, and soft (e.g. polymer) films, z_0 ~10 nm, which is smaller than the typical period of DBRs and photonic cavities designed to manipulate visible light. The maximum reliable experimental displacement and strain amplitudes are u_0~10^{-11} m and η_0~10^{-3} respectively [31,32]. The strain pulses can be considered as picosecond acoustic wavepackets with a broad spectrum of plane acoustic waves, $u \sim e^{-i(\omega t - q_z z)}$, where the dependence of frequency, ω, on the wavevector, q_z, is given by the dispersion relation for acoustic phonons. Thus, for bulk, homogeneous media, $\omega = s_0 q_z$, and in practice the acoustic wavepacket of the picosecond strain pulse is centered at frequencies of 30-100 GHz depending on the quality of the surface and excitation conditions [33].

As the strain pulse propagates through the film, it creates local changes in density which change the permittivity tensor and thus modulate the optical reflectance of the sample. If the thickness of the film is significantly larger than the optical wavelength, then the effect of the strain pulse may be considered qualitatively as an additional source of reflection of an incident probe beam inside the film. The light reflected from the strain pulse then interferes with the light reflected from the surface of the film and the substrate. As the strain pulse propagates through the films, the phase relation between the reflected beams changes periodically between constructive and destructive interference. This results in the output intensity of the reflected probe beam, $I(t)$, oscillating with a period, T, described by the equation [28]:

$$T = \frac{\lambda}{2s_0\sqrt{\varepsilon - \sin^2\theta}}, \quad (2)$$

where ε and θ are the permittivity of the film and the angle of incidence of the probe beam respectively. The oscillations are called Brillouin oscillations because the inverse period T^{-1} is equal to the frequency shift in the Brillouin spectrum for specularly reflected light. The amplitudes of Brillouin oscillations are governed by the changes, $\delta\varepsilon_{ij}$, of the permittivity tensor, ε_{ij}, which for isotropic media may be written as [34]:

$$\delta\varepsilon_{xx} = \delta\varepsilon_{yy} = -\varepsilon_0^{\,2} p_{12}\eta_{zz}$$
$$\delta\varepsilon_{zz} = -\varepsilon_0 p_{11}\eta_{zz} \quad (3)$$

where p_{12} and p_{11} are elasto-optical constants. In addition to the Brillouin oscillations, $I(t)$ will also contain oscillating components due to the change of the total film thickness at times, t, when the strain pulse reaches the substrate and air interfaces of the film [29]. An example of an output signal due to the modulation of the film reflectance by these effects is shown schematically in the inset of Fig. 1(a). It is important to note that Eq. (2) can also be obtained by considering momentum conservation for the interaction between the optical probe beam

#205467 - $15.00 USD Received 24 Jan 2014; revised 21 Mar 2014; accepted 23 Mar 2014; published 13 Jun 2014

and an acoustic plane wave with frequency $\omega = 2\pi T^{-1}$ in the wavepacket of the picosecond strain pulse. The wavevectors of the specularly reflected optical and acoustic waves, **k** and **q** respectively, should fulfill the condition, $q_z = 2k_z$. Including the linear dispersion relations of both the light and sound gives the result obtained in Eq. (2).

If the homogeneous film is replaced by a DBR, the origin of the oscillations in the reflected light becomes more complicated to understand due to the periodically varying nature of the DBR structure. A DBR is defined as being formed by *n* periods comprising two alternating layers with thickness values of d_1 and d_2 and permittivities ε_1 and ε_2 respectively [see Fig. 2(b)]. First, considering the Brillouin oscillations, and using the momentum conservation argument as above, the periodic optical properties of the DBR modify the condition for conservation to give:

$$q_z = 2k_z + \frac{2\pi l}{d_1 + d_2}, \tag{4}$$

where l = 0, ± 1, ± 2… . For l = 0, Eq. (4) reduces to the same condition as for the homogeneous film, but if $l \neq 0$ it is clear that several acoustic harmonics may contribute. Moreover, the presence of both photonic, and potentially, phononic stop bands lead to non-linear dispersion relations. Together, these combined factors act to change the angular dependence of the period of the oscillations relative to that obtained in Eq. (2) and to render it nonlinear with respect to λ.

Secondly, as the strain pulse travels through the DBR, it modulates the position of the internal interfaces between layers. As the position of these interfaces changes, the interference conditions inside the DBR change. This modulates the reflectance of the DBR and leads to further changes in the reflected signal, *I(t)*. These changes are generally not harmonic oscillations and their temporal evolution requires special consideration as discussed below.

The specific tasks of the present work are to characterize the period of Brillouin oscillations in a DBR and to investigate the spectrum of these photoelastically generated oscillations in the DBRs. We deliberately choose a DBR where no acoustic mismatch exists between the layers and concentrate on optical wavelengths in the vicinity of the first PSB. This case is most important in practice when the operating wavelength in nanophotonic devices falls into the PSB of the DBR. As shown below, the main qualitative conclusions obtained from the picosecond acoustic interferometry experiments are shown to be supported by numerical calculations.

3. Experiment

A polymer DBR was prepared on a 50 μm thick, polished Si substrate by spin coating alternating layers of cellulose acetate (CA, Sigma) and poly-9-vinylcarbyzole (PVK, Sigma) from mutually exclusive solvents (diacetone alcohol and chlorobenzene respectively) using a technique similar to that reported previously [35]. The densities of the polymers were ρ_{CA} = 1.3 g cm^{-3} and ρ_{PVK} = 1.2 g cm^{-3} respectively. The resulting structure consisted of 6 repeating polymer bilayers with a 72 ± 1 nm CA film on the bottom and a 65 ± 2 nm PVK film on top (12 layers in total). The individual layer thickness values were measured using a single wavelength self-nulling ellipsometer (λ = 633 nm, 60° angle of incidence). The entire sample was annealed for 12 hours under vacuum (1 mtorr) at 145 °C to remove residual solvent and any stresses that might have been introduced in the multilayer structure during the spin coating procedure.

The permittivities ε_{CA} and ε_{PVK} of the polymers were measured using a spectroscopic ellipsometer (J.A. Woollam Co., Inc., α-SE) and at λ = 400 nm, ε_{CA} = 2.22 and ε_{PVK} = 3.06. Figure 2(a) shows the measured reflectance spectra of the studied DBR at three different angles of incidence, θ. The spectra show a clear photonic stop band near to 400 nm. The wavelength of the centre of the stop band decreases as θ increases. The measured reflectance

#205467 - $15.00 USD Received 24 Jan 2014; revised 21 Mar 2014; accepted 23 Mar 2014; published 13 Jun 2014

spectra show good agreement in the position, width and angular dependence compared to theoretical predictions calculated using an optical transfer matrix method (also shown in Fig. 2(a)). This method used measured thickness and refractive index values of the materials comprising the multilayer to calculate/predict the optical properties of the structure [36].

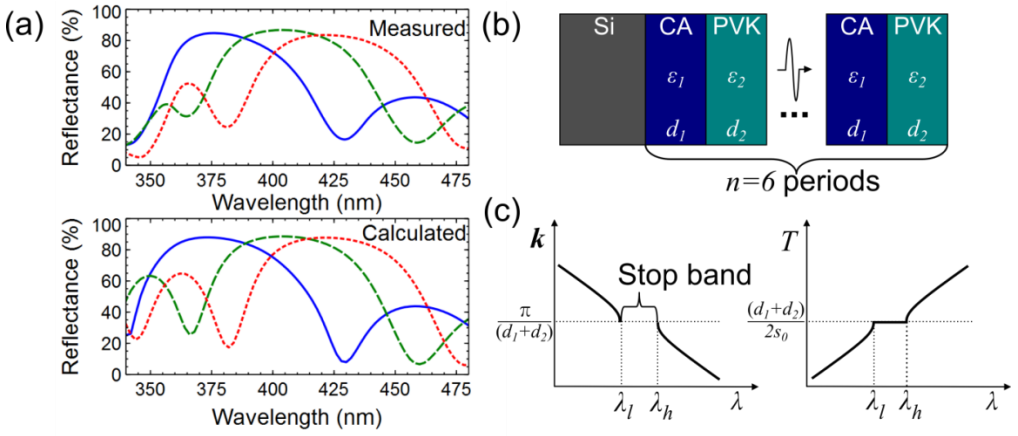

Fig. 2. Reflectance spectra for the DBR studied: (a) measured (top plot) and calculated spectra obtained at angles of 20° (red, dotted line), 35° (green, dashed line), 55° (blue, solid line); (b) a diagram showing the structure of the experimentally measured DBR which consisted of alternating layers of CA and PVK on a Si substrate; (c) the expected optical dispersion relation of a semi-infinite (n = ∞) DBR (left panel) and the period (*T*) of the Brillouin oscillations in DBR in the region of the photonic stop band (right panel).

All of the picosecond acoustic experiments described here were performed at room temperature. Before the DBRs were deposited, an Al film with a thickness of 75 nm had been thermally evaporated on to the back surface of the Si substrate. This Al film was excited using 60 fs optical (pump) pulses from an amplified Ti-sapphire laser (wavelength 800 nm), with a repetition rate of 5 kHz. The pump beam was focused to a 200 μm diameter spot which resulted in the maximum energy density on the Al film being ~10 mJ cm^{-2}. The estimated parameters of the strain and displacement pulses injected into the DBR can be obtained from the scales used in Fig. 1(b).

The high-frequency acoustic properties of the polymers that formed the DBR were studied independently. Single CA and PVK films, 82 ± 1 and 51 ± 2 nm thick respectively, were excited as above, and the coherent oscillations of closed organ-pipe modes in the films were measured [37]. From these, values for the longitudinal sound velocities in the polymers, s_{CA} and s_{PVK}, were obtained. In these films s_{CA} = 2600 ms^{-1} and s_{PVK} = 2400 ms^{-1}, with decay time ~4 ns at ~10 GHz [37,38]. Consequently, the acoustic impedances, $Z_{CA} = \rho_{CA}s_{CA}$ and $Z_{PVK} = \rho_{PVK}s_{PVK}$, of the polymer layers are very close: $Z_{CA} \approx Z_{PVK} \approx 3$ MPa sm^{-1} which allows both reflections of the strain pulse at CA/PVK interfaces and effects related to the phononic stop bands in the DBR to be ignored. In this case, the strain pulse injected into the DBR propagates through the sample without reflections at the interfaces until it reaches the interface of the DBR with the air. There, the strain pulse is reflected with an associated phase change and propagates back towards the Si substrate.

The main goal of the experiments was to measure the temporal evolution of the optical reflectance changes as the strain pulse propagated through the DBR and to attempt to determine the relative contributions of photo-elastic and interface modulation effects. Picosecond temporal resolution was achieved by probing the reflectance of the DBR with a second harmonic (400 nm) optical pulse, originating from the same femtosecond laser that provided the pump beam. The intensity of the reflected probe pulse, $I(t)$, was measured as a

#205467 - $15.00 USD Received 24 Jan 2014; revised 21 Mar 2014; accepted 23 Mar 2014; published 13 Jun 2014

function of *t*, the delay of the probe pulse relative to the pump excitation of the Al transducer. The wavelength of the probing beam, λ = 400 nm, was fixed, so the spectral position of the probe light relative to the PSB of the DBR was controlled by changing the angle θ. In addition, the probe beam could be either *s*- or *p*- polarized.

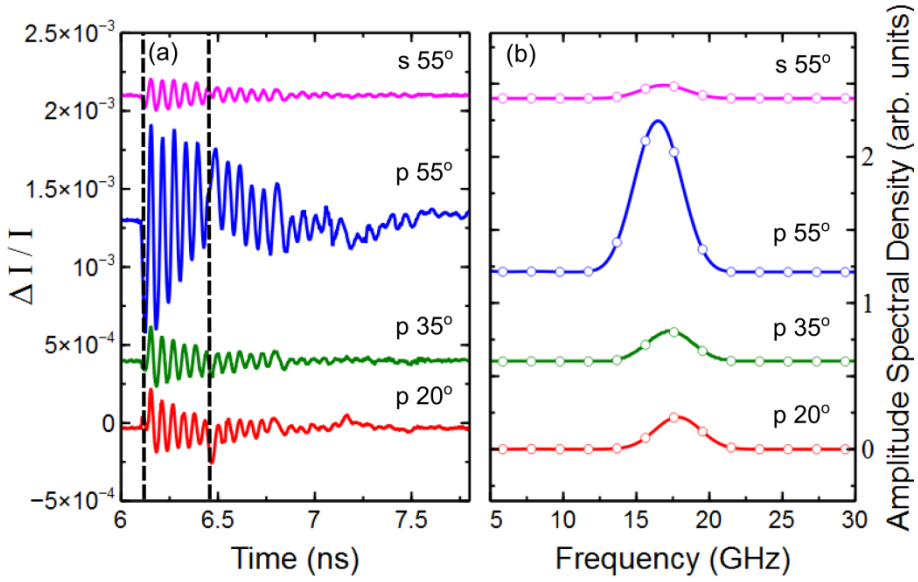

Fig. 3. (a) Examples of the signals obtained in the picosecond acoustic experiments for a variety of polarizations and angles of incidence. (b) Fast Fourier transforms (FFTs, symbols) performed on the signals shown in panel (a) in the time window between the dashed lines. The solid lines in panel (b) are the results of zero-padded FFT's.

The signals, $\Delta I(t)/I_0$, ($\Delta I(t) = I(t)-I_0$, I_0 is the intensity of the reflected light without pump excitation) measured for three values of θ are shown in Fig. 3(a). All signals show oscillations starting at t_1 = 6.11 ns which corresponds to the time it takes for the strain pulse to propagate through the Si substrate. The period *T* of the oscillations varies slightly depending on both θ and the polarization and *I*(*t*) changes abruptly at t_2 = 6.46 ns which corresponds to the time when the strain pulse hits the DBR/air interface. The left and right dashed vertical lines in Fig. 3(a) indicate the values of t_1 and t_2 and thus, the interval where the strain pulse makes its first pass through the DBR. This transient time window, where the oscillations have the highest amplitudes, is the most useful for further analysis because it does not include the phase modulation of *I*(*t*) due to reflections from the Si/DBR and DBR/air interfaces but includes contributions from modulation of the positions of buried interfaces and due to photo-elastic effects. The measured values of t_1 and t_2 allow an estimate of the average sound velocity in the DBR to be obtained as $\bar{s} = n(d_1 + d_2)/(t_b - t_a)$ = 2343 m/s. This is 6% less than the mean sound velocity obtained from the measurements on individual films. This small difference in $\bar{s}$ is likely due to the presence of water in the single CA films when measured compared to the annealed multilayer structure. Single films of CA are known to swell slightly in water vapour. However, CA films capped with PVK layers are protected from swelling by atmospheric water.

Figure 3(b) shows the spectra of the measured signals, $\Delta I(t)/I_0$, obtained by fast Fourier transforming (FFT) the signal in the transient time window between the dashed lines in Fig. 3(a). The spectra show only one line centered at a frequency, *f*, between 15 and 20 GHz that is weakly dependent on the angle θ and the probe beam polarization. There are no other spectral lines in the extended frequency interval from 1 to 100 GHz when the FFT is obtained from

#205467 - $15.00 USD Received 24 Jan 2014; revised 21 Mar 2014; accepted 23 Mar 2014; published 13 Jun 2014

the time interval between the dashed lines in Fig. 3(a). This provides support to the assumption that, for the case presented here, multiple reflections of acoustic waves at the internal interfaces of the DBR may be ignored. If this were not the case, $\Delta I(t)/I_0$ would display beating oscillations, and the spectrum would consist of more than one peak [39]. The width of the spectral line is limited by the width of the time window of the FFT. If a longer time window encompassing the whole signal is used (6 ns < t < 8 ns), then the signal includes the phase shifts of $\Delta I(t)/I_0$ from strain pulse reflection at the DBR/Air and DBR/Si interfaces and eventually detects vibrations of the whole DBR structure, which has a total thickness of 820 nm [37]. FFT's performed in this time window are more complicated than those shown in Fig. 3(b), consisting of several narrow lines that are due to vibrations of the whole multilayer structure and thus will not be addressed further.

The oscillatory behavior of $\Delta I(t)/I_0$ in the DBR sample studied displays similar characteristics to the case of a homogeneous film of a transparent material. As discussed above, the oscillations are the result of the interference of the probe beams reflected from the transient strain pulse, which propagates at the LA sound velocity in the polymers, and those reflected from the surface of the film and CA/Si interface. The task remains to understand the reason for the existence of harmonic oscillations with a single frequency and the absence of higher spectral components which might be expected based upon the predictions of Eq. (4).

4. Discussion and comparison with theory

It is useful to begin by discussing qualitatively what the expected modulation of the signal will be in the ideal case of a DBR with large number of periods (n >>1). Firstly, the photo-elastic effects will be considered by returning to the momentum conservation description of the Brillouin oscillations.

Starting with the condition for momentum conservation from Eq. (4), it is clear that single harmonic oscillations will take place when only the l = 0 mode is present in the signals. This happens when the perturbations to the permittivity tensor, $\delta\varepsilon_{ij}$, are equal throughout the DBR and the dielectric contrast between the individual layers is also small. As such, there will only be one solution for q_z and in an acoustically homogeneous DBR, only a single frequency in the wavepacket of the strain pulse will modulate the reflected light.

When the wavelength, λ, of the light incident on the DBR is far from the PSB, there is no significant difference for the l = 0 mode when compared to the case of a homogeneous film. The period, T, of the oscillations will be accurately described by Eq. (2). When λ falls within the PSB, however, the dependence of T on λ becomes significantly different. This corresponds to wavelengths: $\lambda_l<\lambda<\lambda_h$, where λ_l and λ_h are the optical wavelengths in vacuum that correspond to the lower and upper edges of the PSB respectively (as shown schematically in Fig. 2(c)). Using the momentum conservation condition in Eq. (4), with l = 0, it can be shown that when probing inside the PSB ($\lambda_l<\lambda<\lambda_h$), q_z is independent of λ: $q_z = \mathrm{Re}(k_z) \approx 2\pi/(d_1 + d_2)$. The frequencies, ω, of the acoustic modes that interact with the optical beam are therefore governed by the acoustic dispersion relation, $\omega(\mathbf{q})$. In the present work the acoustic contrast between layers is small and a linear dispersion relation, $\omega = \bar{s}q_z$, where $\bar{s}$ is the mean sound velocity in the DBR, is valid. In this case then, the period of Brillouin oscillations in an ideal DBR with a large number of periods does not depend on λ when $\lambda_l<\lambda<\lambda_h$.

The second effect governing the acousto-optical output of the DBR is modulation of the position of interfaces in the sample. The reflectance of the DBR changes when the strain pulse interacts with the top and bottom interfaces in the DBR (similar to the case of a homogeneous film), but also when the pulse passes internal interfaces between layers. The maximum shift of an interface is typically equal to the amplitude, u_0, of the displacement pulse. For narrow strain pulses ($z_0<<d_1$, d_2) the modulation of the interfaces should result in the appearance of spikes in the temporal evolution of the reflected signal. The time intervals

#205467 - $15.00 USD Received 24 Jan 2014; revised 21 Mar 2014; accepted 23 Mar 2014; published 13 Jun 2014

between the nearest spikes of opposite phase will be equal to the time it takes for the strain pulse to propagate through each layer, d_1/s_1 and d_2/s_2 respectively, and be independent of the probing wavelength λ and incident angle θ.

The numerical analysis presented below has two goals: to provide quantitative support to the qualitative description based on momentum conservation; and to compare the experimental results described above with numerical calculations. The calculations were performed for a DBR with the same parameters as those used in the experiments: the permittivities were $\varepsilon_1 = \varepsilon_{CA} = 2.22$ and $\varepsilon_2 = \varepsilon_{PVK} = 3.06$ at 400 nm; layer thickness values were $d_1 = 72$ nm and $d_2 = 65$ nm for the CA and PVK layers respectively. The optical dispersion of ε_1, ε_2 and the permittivity of Si were taken into account in the calculations. The calculated edges of the PSB for a semi-infinite DBR of these materials are $\lambda_l = 419$ nm and $\lambda_h = 457$ nm. As discussed previously, multiple reflections of the strain pulses at interfaces inside the DBR were not considered and a mean sound velocity inside the DBR, $s = 2343$ m/s, was used.

The numerical calculations of $\Delta I(t)/I_0$ were made using a standard transfer matrix formalism, that accounted for modifications of both the layer thickness and the refractive index due to the strain pulse (photo-elastic effect). The parameters used to model the strain pulse [see Fig. 1(a)] were $z_0 = 10$ nm and $u_0 = 1$ pm respectively. The optical beam was taken to have an infinitely narrow spectral width, which is valid in situations where the spectral width of the probing pulse (3 nm for the experiments here) is smaller than the width of typical spectral features in the DBR's reflectance spectra shown in Fig. 2. The elasto-optical constants [see Eq. (3)] were chosen to be the same in each polymer, so that the perturbations of the permittivity, $\delta\varepsilon_{ij}$, are the same for each layer ($\varepsilon_{CA}^2 p_{12}^{CA} = \varepsilon_{PVK}^2 p_{12}^{PVK} = \beta$). This simplification, which is unlikely to be exactly realized in practice, allows the general properties of the acousto-optical effects caused by $l = 0$ mode inside DBRs to be understood.

The signals, $\Delta I(t)/I_0$, were calculated as a function of the probing wavelength, λ, in order to show how close the dependence of the oscillation period T on λ in real DRBs is to the case when $n = \infty$. $\Delta I(t)/I_0$ was calculated for $n = 6$, at three values of λ, corresponding to the center ($\lambda = \lambda_c$) and each edge of the PSB ($\lambda = \lambda_l$, and λ_h). To demonstrate the effect of each mechanism for acousto-optical modulation, two extreme cases for the strength of the photoelastic effect are shown: $\beta = 0$ [Fig. 4(a)] and $|\beta| = 200$ [Fig. 4(b)]. These correspond to purely interface displacement driven modulation and to a dominantly photoelastic modulation respectively. The temporal evolution of $\Delta I(t)/I_0$ in these two cases is very different: the signal induced by interface displacement is strongly anharmonic and the position of the peaks in the signal does not depend on λ; the signal dominated by photo-elastic mechanisms is harmonic and the period, T, of the oscillations appears to depend slightly on λ.

#205467 - $15.00 USD Received 24 Jan 2014; revised 21 Mar 2014; accepted 23 Mar 2014; published 13 Jun 2014

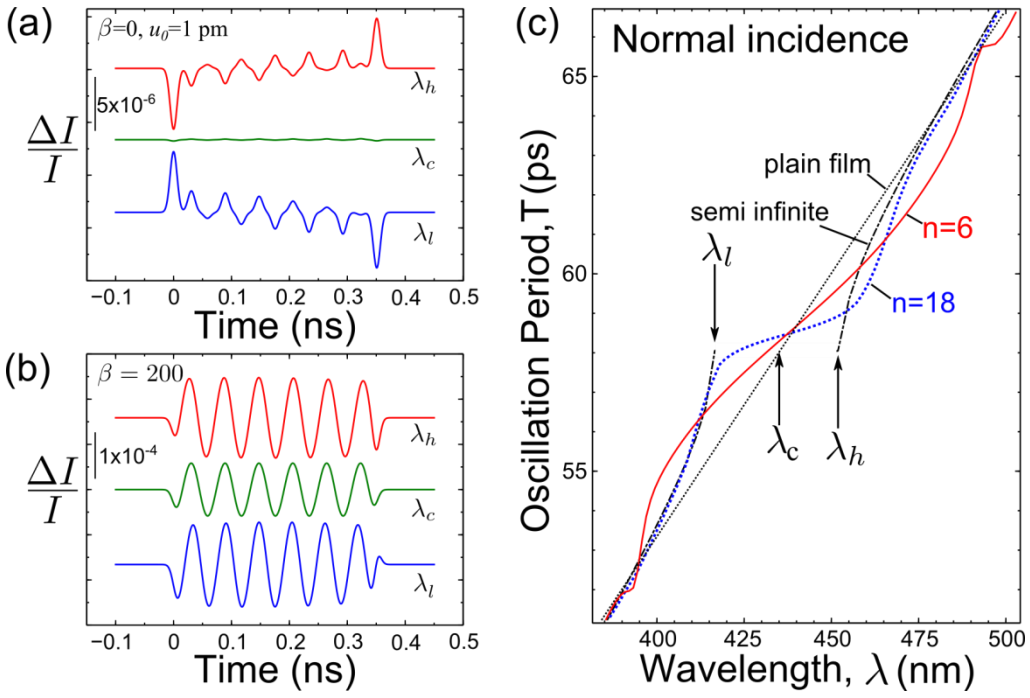

Fig. 4. (a) Calculated intensity signals at different wavelengths of incident light for the DBR studied here. These calculations consider only the changes in structure due to displacement of internal interfaces. (b) Calculated intensity signals for the same DBR when photoelastic effects dominate the optical response of the structure i.e. β is large. The results of calculations are shown for optical probe wavelengths at the centre ($\lambda = \lambda_c$) and edges ($\lambda = \lambda_l$ and $\lambda = \lambda_h$) of the PSB. (c) The results of calculations of the optical wavelength dependence of the oscillation period, T, for increasing numbers of layers in the DBR. As expected, when the number of layers increases, the dependence of T tends towards to the case for a semi-infinite DBR.

The amplitude of $\Delta I(t)/I_0$ when probing at the center of the PSB ($\lambda = \lambda_c$) is less than when probing at the edges. It is obvious that in the semi-infinite PSB, when the reflectance is 100% for $\lambda_l<\lambda<\lambda_h$, the amplitude of the signal will be zero for both mechanisms. For the finite number of periods there will be always non-zero modulation but as shown in Figs. 4(a) and 4(b) the difference in the amplitudes between probing with λ inside and outside the PSB is very different for two mechanisms: for the changes of the reflectance induced by the displacement of the interfaces the amplitude decreases by a factor of ~40-50 when probing in PSB of the DBR with n = 6; when considering only the photoelastic mechanism in the same PSB the amplitude of $\Delta I(t)/I_0$ is a factor of two smaller than when probing at the edges . The slight dependence of T on λ in the region of the PSB appears contrary to the qualitative discussion above. It is, however, a consequence of the fact that this calculation is for a real DBR, with a finite number of layers. Figure 4(c) shows the dependence of the oscillation period, T, on λ for DBRs with different numbers of layers (n = 6, n = 18) in the case where the photoelastic effect is dominant ($|\beta| >> 1$). These calculations are compared to a curve corresponding to a semi-infinite DBR. The dashed-dotted line corresponds to a homogeneous film with ε = 2.62. It can be seen that in the vicinity of the PSB, for n = 6, $T(\lambda)$ already differs by several percent relative to the homogeneous film. As n increases, T becomes increasingly sensitive to λ at the very edges of the stop band (λ_l and λ_h) while the dependence inside the stop band decreases. As expected, further increasing n results in $T(\lambda)$ approaching the case of the semi-infinite DBR.

These results serve to show that the calculations support the qualitative description of the influence of the PSB on the properties of Brillouin oscillations due to the photoelastic effect

#205467 - $15.00 USD Received 24 Jan 2014; revised 21 Mar 2014; accepted 23 Mar 2014; published 13 Jun 2014

in a DBR. In the given example, when the photoelastic mechanism is dominant, the difference in T in a DBR relative to a homogeneous film is only several percent even when $n = \infty$. If, however, the materials of the DBR are chosen so that the elasto-optical properties are significantly different in each layer (i.e. $\varepsilon_{CA}^2 p_{12}^{CA} \neq \varepsilon_{PVK}^2 p_{12}^{PVK}$), calculations (results not shown) indicate that the reflected signals will consist of several harmonics and the difference in the optical response becomes large when a picosecond strain pulse is applied to the DBR rather than a homogeneous film.

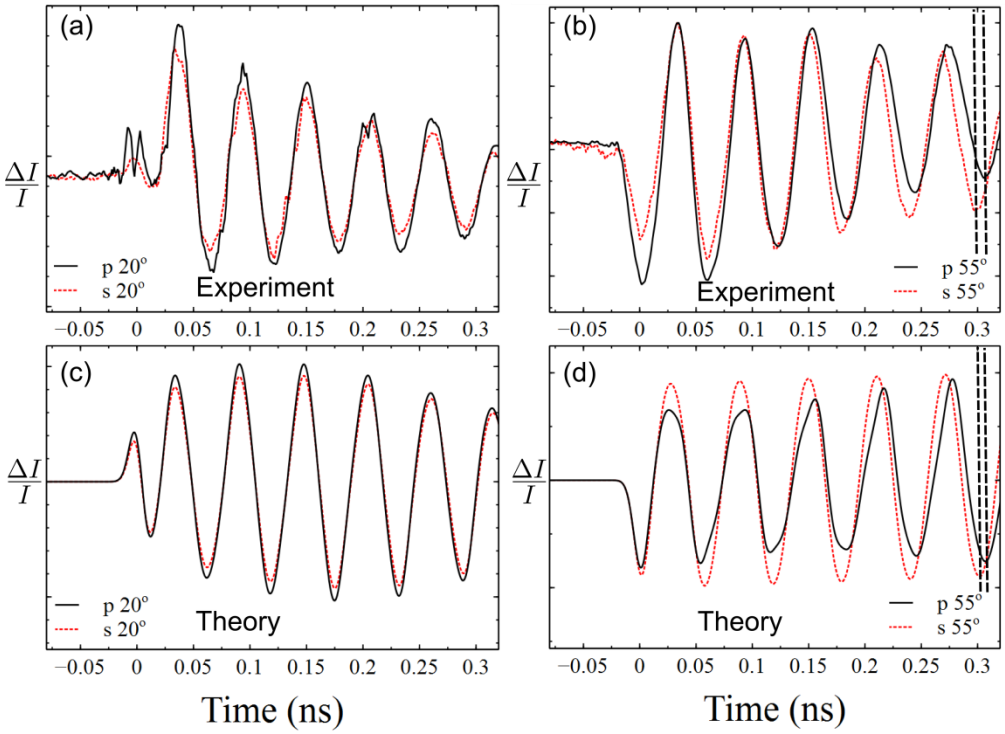

Fig. 5. Measured (a, b) and calculated (c, d) reflected intensity signals for both s (dotted red line) and p (solid black line) polarizations of probe light at angles of incidence of 20° [(a), (c)] and 55° [(b), (d)]. The calculated signals reproduce the key features of the measured signals supporting the validity of the theoretical approach applied to modelling the optical response of the DBR. The dashed vertical lines in (b) and (d) highlight the shifts in the oscillation period that are observed between the p and s components of the reflected light intensity (see text).

The results show that the FFTs of the experimentally measured signals [see Figs. 3(a) and 3(b)] in the time interval $t_1<t<t_2$ are well described by a single spectral line. Thus, based on the theory above, it may be concluded that the photoelastic effect is sufficient to describe the experimentally observed acousto-optical modulations and only the fundamental ($l = 0$) mode is active in forming the reflectance signal. From a comparison of the measured and calculated amplitudes and phases of the oscillations in the signals at $\lambda = 400$ nm, for various values of θ and both s and p polarizations it is estimated that the elasto-optical constants: $p_{12}^{CA} \sim p_{12}^{PVK} \sim p_{11}^{CA} \sim p_{11}^{PVK} \sim 1$.

To convince of the agreement between calculations and experiment it is possible to make a comparison between the temporal evolution of measured and calculated for $p_{12}^{CA} = p_{12}^{PVK} = p_{11}^{CA} = p_{11}^{PVK} = 1$ signals $\Delta I(t)$. Figure 5 shows the measured and calculated signals for both s- and p-polarizations at two separate angles of incidence, corresponding to probing on each edge of the stop band. Both the experimental [Figs. 5(a) and 5(b)] and

#205467 - $15.00 USD Received 24 Jan 2014; revised 21 Mar 2014; accepted 23 Mar 2014; published 13 Jun 2014

theoretical [Figs. 5(c) and 5(d)] curves show oscillations close to harmonic waveforms and are found to be in good agreement. For $\theta = 20°$ the signals $\Delta I(t)$ for different polarizations are almost the same. A small but distinguishable difference in values of T for *s*- and *p*- light is seen at the higher angle of incidence (Figs. 5(b) and 5(d)). This difference is noticeable in both, experimental and theoretical, curves when comparing the temporal positions of maxima/minima in $\Delta I(t)$ at the times corresponding to 4th and 5th oscillations. It is important to note that this difference, indicated by vertical dashed lines in Figs. 5(b) and 5(d), for *s*- and *p*-light is not due to optical anisotropy induced by the strain pulse because the model assumes that $\delta\varepsilon_{xx} = \delta\varepsilon_{yy} = \delta\varepsilon_{zz}$ but is due instead to the differences in the angular dependence of the p and s reflection coefficients. This difference is not present at the lower angle of incidence due to the fact that the *p* and *s* reflection coefficients for dielectric interfaces are similar close to normal incidence. In both cases, there is good agreement between the periods obtained for the measured and calculated signals. Theoretical $\Delta I(t)$ curves for the *p* polarization show small anharmonic features as shown in Fig. 5(d) (black solid curve), which are due to the larger contribution of the interface modulation effects for large incident angles. These anharmonic features are not seen in the experimentally measured $\Delta I(t)$ [Fig. 5(b)] due to the limited signal to noise ratio in the experiments.

In the above discussion we have attributed the absence of modes with $l>0$ to the dominance of the photoelastic effect. Another reason for damping of higher harmonics in $\Delta I(t)/I_0$ could be due to strong attenuation of high-frequency acoustic components in the strain pulse wavepacket while it propagates in the polymer film. We note, however, that the mean free path for these high frequency phonons is larger than the period of the DBR [37,38]. This would mean that when the strain pulse passed the first few layers in the DBR (from the substrate side) anharmonic features would be noticeable in the temporal evolution of $\Delta I(t)$. This is not observed experimentally and we may therefore conclude that anharmonic modulations due to modes with $l>0$ and the displacement of the interfaces of the DBR are relatively weak in the DBR studied here.

5. Conclusions

In summary, the reflected signals, $\Delta I(t)/I_0(t)$, induced by the picosecond strain pulse are shown to be close to harmonic when the photoelastic effect is the dominant mechanism of reflectance modulation and only the fundamental $l = 0$ mode is active. For the DBR studied in the present work, the modulated signals may be characterized by a single period, T, with a value close to that expected in a homogeneous film with a mean permittivity ε. The model calculations show that the angular and wavelength dependencies of this period are suppressed slightly when probing in the region of the PSB relatively to the plain film. The amplitude of the modulation depends on the position of the probe wavelength λ relative to the PSB. In DBRs with a large number of layers, n, modulations due to both the photo-elastic effect and interface displacement become negligible when λ lies in the PSB. When n is not so high, modulations due to interface displacement are negligible when $\lambda = \lambda_c$ but those due to the photo-elastic effect are still obvious in the signals. The semi-quantitative agreement between the measured and calculated signals and the success of the theoretical approach used in reproducing specific features of the signals from the DBRs suggests that the model captures the essential physics of optical modulation in these samples.

For the polymer sample structure considered here, the picosecond strain pulse induces only small changes in the reflectance of the DBR. In fact, the maximum amplitude of $\Delta I(t)/I_0(t)$ is less than 1% and does not differ significantly from the case of a homogeneous film. Despite its weak acousto-optical response, if the DBR is used as an element in an active device (e.g. a vertical-cavity surface–emitting laser), even small changes in the reflectance could result in large changes in the optical output and mode structure of the laser device [40]. We also note that the weak optical response from the DBR would be favourable for some

#205467 - $15.00 USD Received 24 Jan 2014; revised 21 Mar 2014; accepted 23 Mar 2014; published 13 Jun 2014

applications. For example, it was recently proposed that strong photon-phonon interactions in optical microcavitites formed using DBRs can be used for light modulation in optoelectronic devices [15,40–42]. In this case the modulation takes place in the cavity layer and any acousto-optic effects in the DBRs should be minimal. On the other hand, a DBR with high photoelastic constants could be used for efficient modulation and clocking of the optical signals. The important difference between homogeneous films and DBRs is that it would be possible to generate higher acoustic harmonics using DBRs. Therefore, the approach presented in our work may be applied to the engineering of various nanophotonic devices based on DBRs where efficient GHz modulation of light using acousto-optical effects is required.

Acknowledgments

The authors wish to thank Dr. Vladimir Korolkov for assistance with the spectroscopic ellipsometry measurements. Financial support for this project was provided by the Engineering and Physical Sciences Research Council (EPSRC) under grant numbers EP/G035202/1 and EP/H004939/1.

#205467 - $15.00 USD Received 24 Jan 2014; revised 21 Mar 2014; accepted 23 Mar 2014; published 13 Jun 2014